Structure of confined water

2001 J. Phys.: Condens. Matter 13 9165

(http://iopscience.iop.org/0953-8984/13/41/308)

INSTITUTE OF PHYSICS PUBLISHING JOURNAL OF PHYSICS: CONDENSED MATTER

J. Phys.: Condens. Matter **13** (2001) 9165–9177 PII: S0953-8984(01)28360-X

Structure of confined water

M-C Bellissent-Funel

Laboratoire Léon Brillouin (CEA-CNRS), CEA-Saclay, 91191 Gif-sur-Yvette, France

E-mail: mcbel@llb.saclay.cea.fr

Received 29 August 2001
Published 28 September 2001
Online at stacks.iop.org/JPhysCM/13/9165

Abstract

Water is essential for the stability and function of biological macromolecules. In living systems, essential water-related phenomena occur in restricted geometry in cells, and at active sites of proteins and membranes or at their surface. In this paper, we present the more recent results on the structure of confined water as compared with that of bulk supercooled water. In particular, the combined effects of the hydration level and the temperature on the change of the structure of water are discussed in the light of powerful techniques.

1. Introduction

In many technologically important situations, water is not in its bulk form but is instead attached to substrates or filling small cavities. Common examples are: water in porous media, such as rock or sandstones; and water in biological materials, such as in the interior of cells or attached to surfaces of biological macromolecules and membranes. This is what we define here as 'confined' or 'interfacial water'. Water in confined space has attracted considerable interest in the last few years [1]. It is commonly believed that the structure and dynamics of water are modified by the presence of solid surfaces, both by a change of hydrogen bonding and by modification of the molecular motion that depends on the distance of water molecules from the surface.

This paper accounts for the more recent results on the microscopic structure of confined water as a function of temperature. We report on some unusual nucleation and structural properties of water, on one hand, confined in a porous hydrophilic silica glass and, on the other hand, in contact with a hydrophobic surface, namely activated carbon. Finally, the effect of hydration and temperature on water–protein interactions is discussed.

2. Theory

According to the static approximation of neutron scattering theory [2], the structure factor of a molecular liquid $S_M(Q)$ is related to the distinct part (terms $i \neq j$) of the differential scattering

cross section $(\mathrm{d}\sigma/\mathrm{d}\Omega)^{\mathrm{distinct}}$. So, for heavy water,

$$S_M(Q) = \left[\left(\frac{\mathrm{d}\sigma}{\mathrm{d}\Omega}\right)^{\mathrm{distinct}} + (b_{\mathrm{O}}^2 + 2b_{\mathrm{D}}^2)\right] \Big/ (b_{\mathrm{O}} + 2b_{\mathrm{D}})^2 \tag{1}$$

where b_{O} and b_{D} are the coherent scattering lengths of oxygen and deuterium, respectively.

For a molecular liquid, the structure factor may be split into two parts:

$$S_M(Q) = f_1(Q) + D_M(Q) \tag{2}$$

where $f_1(Q)$ is defined as the molecular form factor and the $D_M(Q)$ function contains only the intermolecular contributions. Thus, at large Q ($Q > 8$ Å^{-1}), the main contribution to $S_M(Q)$ comes from $f_1(Q)$ whereas $D_M(Q)$ goes to zero.

The $D_M(Q)$ function is Fourier transformed in order to get the pair correlation function $g_L(r)$ for the intermolecular terms only. $g_L(r)$ is related to the $d_L(r)$ function by

$$d_L(r) = 4\pi\rho_M(g_L(r) - 1) = \frac{2}{\pi}\int_0^\infty Q D_M(Q) \sin Qr \, \mathrm{d}Q \tag{3}$$

where ρ_M is the number density. For pure D_2O, $g_L(r)$ is a weighted sum of the partial pair correlation functions g_{OD}, g_{DD} and g_{OO}, namely

$$g_L(r) = 0.489 g_{\mathrm{DD}}(r) + 0.421 g_{\mathrm{OD}}(r) + 0.090 g_{\mathrm{OO}}(r). \tag{4}$$

Let us note that the main contributions to $g_L(r)$ come from the DD and OD correlations. This is the reason for which neutron and x-ray structure factors are combined to determine more precisely the pair partial functions [3, 4]. Moreover, in the low-r range ($0 < r < 1.5$ Å), the peaks due to the intramolecular distances are not present in the $d_L(r)$ and $g_L(r)$ functions. This property has been used in the data analysis (see reference [5]).

3. Experimental procedure

We recall here the method that we adopted to determine the neutron structure factor $S_M(Q)$ of heavy water (D_2O) [5]. Experiments have been performed on the 7C2 spectrometer of the Orphée reactor of the Laboratoire Léon Brillouin, at Saclay (France), for a momentum transfer Q ranging between 0.5 and 16 Å^{-1} ($Q = (4\pi/\lambda)\sin(\theta/2)$, $\lambda = 0.705$ Å and $2\theta_{max} = 128^\circ$). According to equation (2), the structure factor $S_M(Q)$ is given by $S_M(Q) = D_M(Q) + f_1(Q)$ where

$$\begin{aligned} D_M(Q) = \frac{1}{(b_{\mathrm{O}} + 2b_{\mathrm{D}})^2}\big[\big\{&(1/K)I_{cor}(Q) - A - BQ^2 - CQ^4 + b_{\mathrm{O}}^2 + 2b_{\mathrm{D}}^2\big\} \\ &- \big\{b_{\mathrm{O}}^2 + 2b_{\mathrm{D}}^2 + 4b_{\mathrm{O}}b_{\mathrm{D}} j_0(Q_{eff}r_{\mathrm{OD}}) \exp(-\gamma_{\mathrm{OD}}Q_{eff}^2) \\ &+ 2b_{\mathrm{D}}^2 j_0(Q_{eff}r_{\mathrm{DD}}) \exp(-\gamma_{\mathrm{DD}}Q_{eff}^2)\big\}\big] \end{aligned} \tag{5}$$

$$\begin{aligned} f_1(Q) = \frac{1}{(b_{\mathrm{O}} + 2b_{\mathrm{D}})^2}\big[\big\{&b_{\mathrm{O}}^2 + 2b_{\mathrm{D}}^2 + 4b_{\mathrm{O}}b_{\mathrm{D}} j_0(Q_{eff}r_{\mathrm{OD}}) \exp(-\gamma_{\mathrm{OD}}Q_{eff}^2) \\ &+ 2b_{\mathrm{D}}^2 j_0(Q_{eff}r_{\mathrm{DD}}) \exp(-\gamma_{\mathrm{DD}}Q_{eff}^2)\big\}\big]. \end{aligned} \tag{6}$$

In equation (5), $I_{cor}(Q)$ is the intensity of the sample corrected for self-absorption effects. The normalization factor K and the coefficients A, B, C of the polynomial expansion which allows one to correct for the inelasticity effect are obtained using the fitting procedure as described in reference [5]; r_{OD} and r_{DD} are respectively the intramolecular oxygen–deuterium and deuterium–deuterium distances, γ_{OD} and γ_{DD} are the Debye–Waller factors due to the internal vibrations of the molecule and $j_0(x) = \sin(x)/x$ is the zeroth-order spherical Bessel function.

At $Q = 0$, $I_{cor}(0)$ and $S_M(0)$ are connected via the following equation:

$$S_M(0) = \left[(1/K)I_{cor}(0) - A + b_O^2 + 2b_D^2\right]/(b_O + 2b_D)^2. \quad (7)$$

In the fitting procedure, $I_{cor}(0)$ is calculated using the value of $S_M(0)$ deduced from the following relation: $S_M(0) = \rho_M k_B T \chi_T$ using the values of the number density ρ_M and the isothermal compressibility χ_T of heavy water [5].

4. Microscopic structure of bulk water

The structural properties of water have now mostly been well explained in some range of temperatures and pressures using different techniques including molecular dynamics and Monte Carlo simulations [3–8].

The number of models of its structure is very large and the number of experimental results enormous. The reason for such interest lies in the fact that water has unusual physical and chemical properties due mainly to the presence of H bonds. The phase diagram of water [9] exhibits a remarkable polymorphism as shown in figure 1. Besides all these crystalline phases, one must add two amorphous solids: low-density amorphous (LDA) ice and high-density amorphous (HDA) ice. The microscopic structures of these two forms of amorphous ice have been studied by means of both x-ray [10] and neutron scattering [1–12]. In this paper, we compare the structure of confined water with that of supercooled water and amorphous ice.

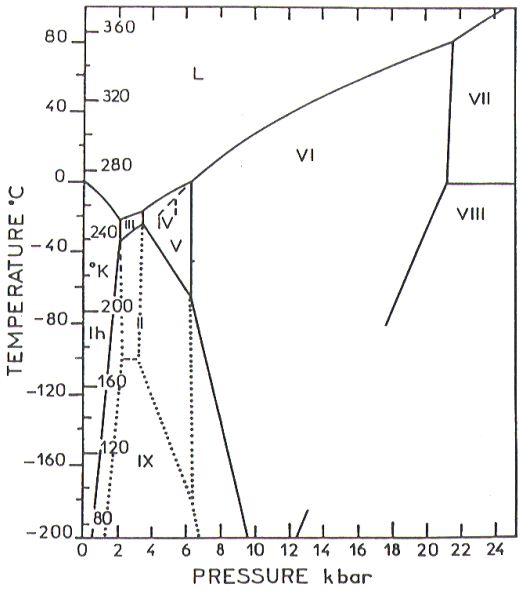

Figure 1. The phase diagram of water [9].

4.1. Structure factors $S_M(Q)$ of supercooled water

In order to supercool water, we used D_2O/deutero-heptane/CCl_4/Sorbitan emulsions [13, 14]. Figure 2 gives the structure factors $S_M(Q)$ of supercooled water [13] at $-10.5\,^{\circ}C$ and $-31.5\,^{\circ}C$, as compared with that of low-density amorphous ice. When the temperature is decreased it appears that the main peak position Q_0 of the structure factor of supercooled water tends towards the value of 1.69 Å^{-1} that is characteristic of low-density amorphous ice [11].

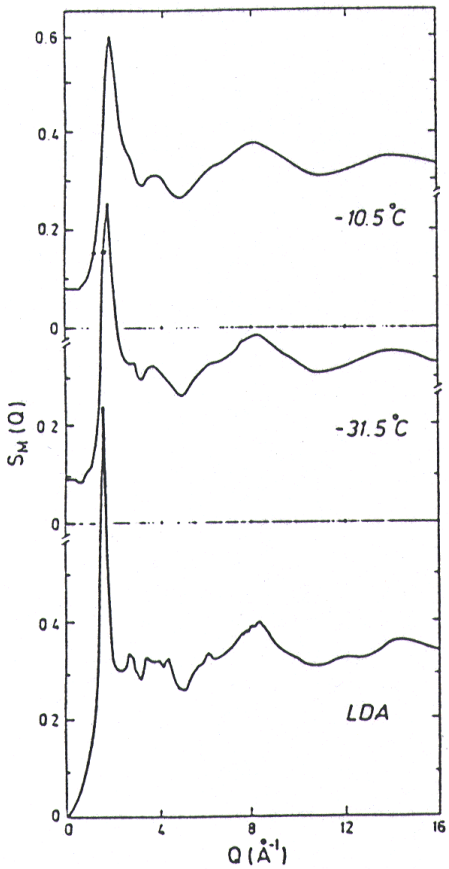

Figure 2. Structure factors $S_M(Q)$ of supercooled D_2O, at normal pressure, as compared with that of low-density amorphous ice (LDA) at 77 K [11].

4.2. Pair correlation functions $d_L(r)$ of supercooled water

The composite pair correlation functions $d_L(r)$ of supercooled water at $-10.5\,^{\circ}$C and $-31.5\,^{\circ}$C [13] are displayed in figure 3 and compared with that of low-density amorphous ice [11].

At $-31.5\,^{\circ}$C, in the small-r range of $d_L(r)$, some features characteristic of low-density amorphous ice become apparent. In particular, the O–D hydrogen bond distance at 1.82 Å and the D–D intermolecular distance at 2.31 Å are present. In the large-r range of $d_L(r)$, one observes additional small oscillations which are not present at $-10.5\,^{\circ}$C and an out-of-phase behaviour of the broad oscillations for values of r higher than 10 Å. These features are similar to those observed in low-density amorphous ice.

At normal pressure and low temperature, the measurements confirm the increasing spatial correlations in deeply supercooled water as the temperature is decreased and the tendency to evolve towards the structure of low-density amorphous ice. In supercooled water, the structure present between 4.5 and 6.0 Å is connected to the formation of tetrahedrally coordinated patches. It is clear that such patches are not present in the high-pressure liquid water, either because the hydrogen bonds are broken, i.e. the molecular energy is on average too low or, more likely, because the hydrogen bond network is distorted.

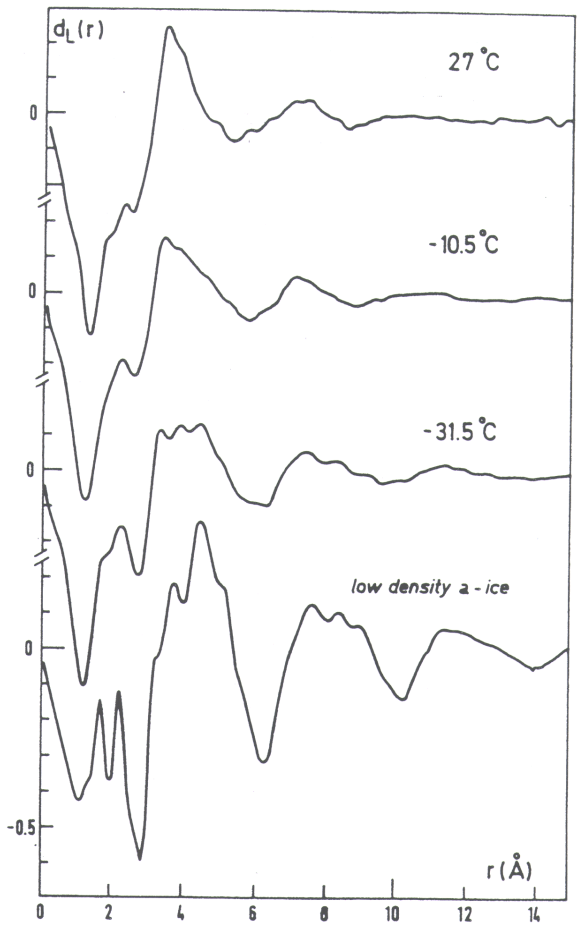

Figure 3. The weighted pair correlation function $d_L(r)$ of liquid D_2O at different temperatures as determined by neutron scattering; the comparison is with low-density amorphous ice [11].

5. Microscopic structure of confined water

5.1. Model systems with hydrophilic interactions

The choice of porous media as model systems depends on the following conditions: a well-characterized pore size distribution and a knowledge of surface details. The structure of confined water has been studied in many hydrophilic model systems by means of neutron diffraction; let us mention clay minerals [15, 16], and various types of porous silica [17–22]. In the last case, the results were interpreted in terms of a thin layer of surface water with more extensive H bonding, lower density and mobility and lower nucleation temperature as compared to bulk water.

Recent results concern the structure of water confined in a Vycor glass. Vycor is a porous silica glass, characterized by a quite sharp distribution of cylindrical interconnected pores, and hydrophilic surfaces. Results have been obtained as functions of the level of hydration h (given in grams of water/grams of dry Vycor) from full hydration 100% ($h = 0.25$) down to 25% ($h = 0.0625$) and temperature [23–25].

Vycor-brand porous glass No 7930 is a product of Corning Glass Works [26]. It is made by heating a homogeneous mixture of boron oxide glass and silica above the melting point and then quenching this mixture to a temperature below the spinodal line where the mixture phase separates into two mutually interpenetrating regions. At a certain stage of preparation, the boron-rich region is leached out by acid, leaving behind a silica skeleton with a given distribution of pore sizes (see figure 4). The average pore diameter in Vycor 7930 is 50 Å, as stated by the manufacturer.

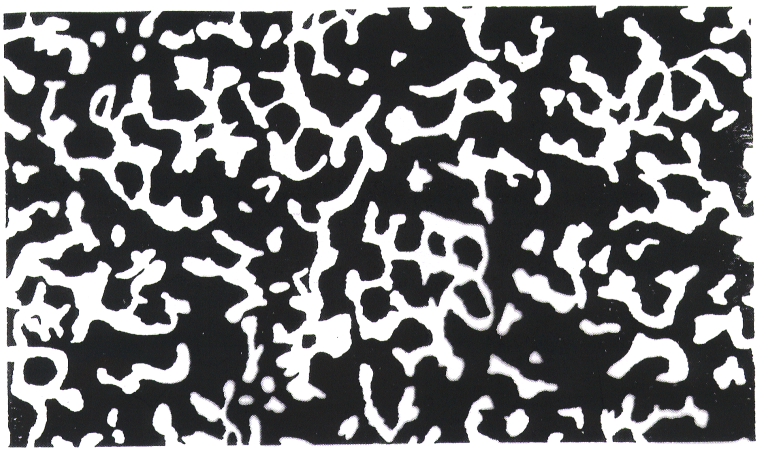

Figure 4. An image of the pore network in Vycor of mean pore diameter 50 Å, based on a transmission electron micrograph (from [50], used with permission).

We adopted the following procedure for the preparation of the Vycor samples. The Vycor rods were immersed in 30% hydrogen peroxide and heated to 90 °C for a few hours to remove any organic impurities absorbed by the glass. The Vycor was then washed several times in distilled water in order to remove the hydrogen peroxide and stored in distilled water. When a hydrated Vycor sample is heated at 90 °C in vacuum until it is dry, it becomes translucent and clear, defining what we called a 'dry Vycor sample'. At full hydration, a Vycor glass absorbs water up to 25% of its dry weight. A partially hydrated sample is then obtained by absorption of water in the vapour phase until the desired level of hydration is reached. The sample that we used in this experiment was hydrated by D_2O to a level of 25% (i.e. 0.0625 grams per gram). This hydration corresponds to one-monolayer coverage. The sample consists of a hydrated Vycor rod of diameter 7.9 mm put in a cylindrical vanadium container. Based on the information that the density of dry Vycor is 1.45 g ml^{-1}, the porosity 28% and the internal cylindrical pores of cross sectional diameter 50 Å, a 50%-hydrated sample has three layers of water molecules on its internal surface. A 25%-hydrated sample corresponds roughly to one-monolayer coverage of water molecules.

The $d_L(r)$ pair correlation functions are displayed in figure 5 for two levels of hydration of Vycor. The $d_L(r)$ function for water from a fully hydrated sample (figure 5(a)) is almost identical to that of bulk water (figure 5(c)) [23, 24]. In the case of a partially hydrated sample (figure 5(b)), the difference with respect to bulk water (figure 5(c)) is small. However, the three site–site radial correlation functions are definitely required for a sensible study of the orientational correlations between neighbouring molecules. They have been obtained from three neutron diffraction experiments on three different isotopic mixtures of light and heavy water [27] and compared with the results of molecular dynamics simulations [28].

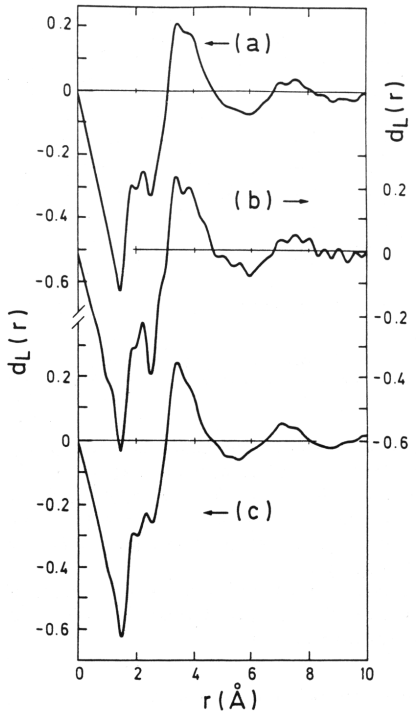

Figure 5. $d_L(r)$ for (a) confined D_2O from fully hydrated Vycor (27 °C) and (b) confined D_2O from partially hydrated Vycor (35 °C) compared with (c) bulk water (27 °C) [4].

Nevertheless, the evolution of the total intensity $I(Q)$ as a function of temperature is of great interest. In effect, we have shown that the temperature of nucleation of water in Vycor decreases with the level of hydration. For a 50%-hydrated sample, the deepest supercooling temperature is −27 °C, while for the fully hydrated sample it is −18 °C. As the temperature goes below the limit of supercooling, the Bragg peaks of ice appear. It is worth noting that, in Vycor, water always nucleates into cubic ice (figure 6(a)) which is in sharp contrast to the case for bulk water that always nucleates into hexagonal ice. The nucleation of cubic ice can be explained in terms of distortion of the microscopic structure of water confined in a hydrophilic substrate. It seems that the confinement of the water favours the nucleation of cubic ice, which appears superimposed on the spectrum of liquid water and whose proportion can be deduced from the intensity of the (111) Bragg peak. The proportion of cubic ice increases with decreasing temperature. In fact, at −100 °C, the spectrum of confined water looks similar to that of cubic ice (figure 6(a)). In figure 6(b), we show a spectrum of confined D_2O, at −18 °C, from fully hydrated Vycor, after subtraction of the Bragg peaks of cubic ice. This gives clear evidence that liquid water is still present at −18 °C; there is about 23% of liquid water.

The results relevant to a 25%-hydrated Vycor sample indicate that, at room temperature, interfacial water has a structure similar to that of bulk supercooled water, at a temperature of about 263 K which corresponds to a shift of 30 K [25]. The structure of interfacial water is thus characterized by an increase of the long-range correlations which corresponds to the building of the H-bond network as it appears in low-density amorphous ice [11]. There is no evidence of ice formation when the sample is cooled from room temperature down to −196 °C (liquid nitrogen temperature) [25].

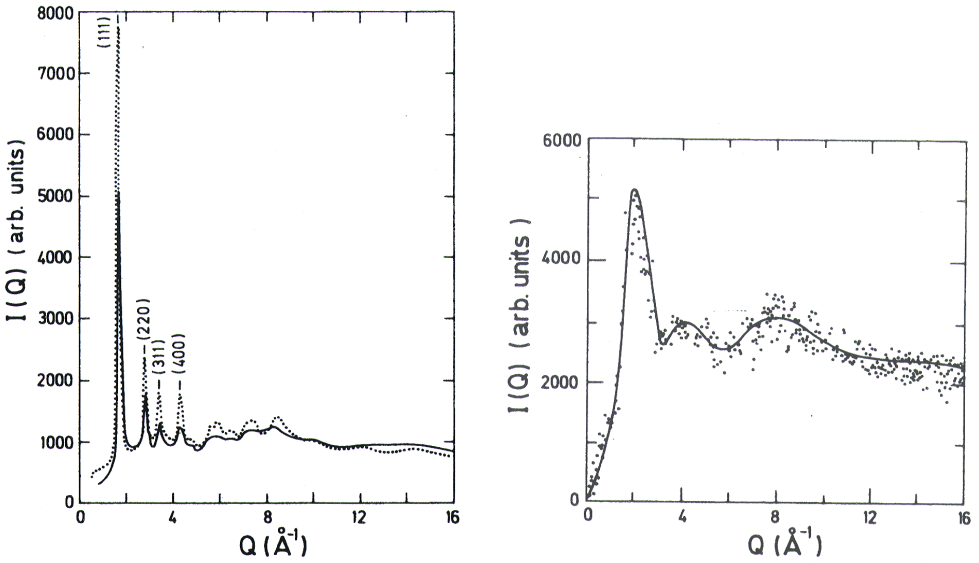

(a) (b)

Figure 6. (a) The spectrum of cubic ice at −198 °C (dotted line) compared with that of confined D_2O at −100 °C from fully hydrated Vycor (full line) [23]. (b) The spectrum of confined D_2O at −18 °C from fully hydrated Vycor after subtraction of Bragg peaks. There is 23% of liquid water [23].

5.2. Model systems with hydrophobic interactions

Among those of hydrophobic model systems, one experimental investigation of particular interest concerns the structure of water in contact with an activated charcoal powder from Aldrich Chemical Company (<100 mesh) [29]. Scanning electron micrographs of the material (figure 7) give an idea of the size of the specks and their distribution. The porosity and the specific surface of the powder have been determined using the Brunaumer–Emmet–Teller (BET) technique. The data summarized in table 1 show that two sets of pores exist in the sample; the mesopores occupy 82% of the space, while the remainder is composed of micropores.

Table 1. Characteristic properties of the carbon powder (BET).

	Mean pore diameter (Å)	Pore volume ($cm^3\ g^{-1}$)	Specific surface area ($m^2\ g^{-1}$)
Mesopores	35	1.08	1487
Micropores	10	0.135	280

The microscopic structure of confined water has been determined by means of both x-ray and neutron diffraction, as functions of hydration and temperature, from room temperature down to 77 K. We comment only on the results relevant to the lowest water content (42%), because at the highest water content (≈200%), the structure of water in carbon powder is identical to that of bulk water. The pair correlation functions $d_L(r)$ obtained by x-ray measurements are shown in figure 8 (solid lines) together with the curve related to bulk water (dotted line). To a good approximation, x-ray measurements yield mainly information about the oxygen–oxygen distribution function. At the lowest water content (figure 8(b)), the local

Figure 7. A scanning electron micrograph of dry carbon powder [29].

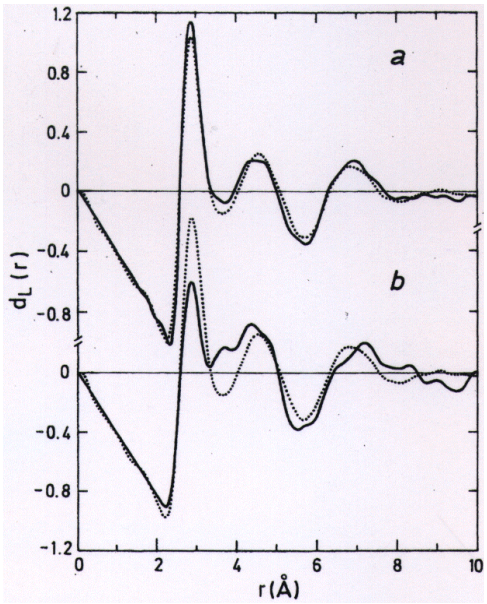

Figure 8. The x-ray pair correlation function $d_L(r)$ of water contained in activated carbon, at room temperature, shown by solid lines for 188% (curve a) and 42% hydration (curve b). For comparison, the $d_L(r)$ curve of bulk water at the same temperature is also shown in each case (dotted lines) [29].

environment exhibits noticeable modifications which are interpreted as a distortion of the tetrahedral ordering in confined water. Neutron scattering experiments have been analysed in terms of intermolecular functions $d_L(r)$ (figure 9): at the same low water content (42%), it appears that the first peak of the $d_L(r)$ function, related to the D $\cdots$ O distance, is higher,

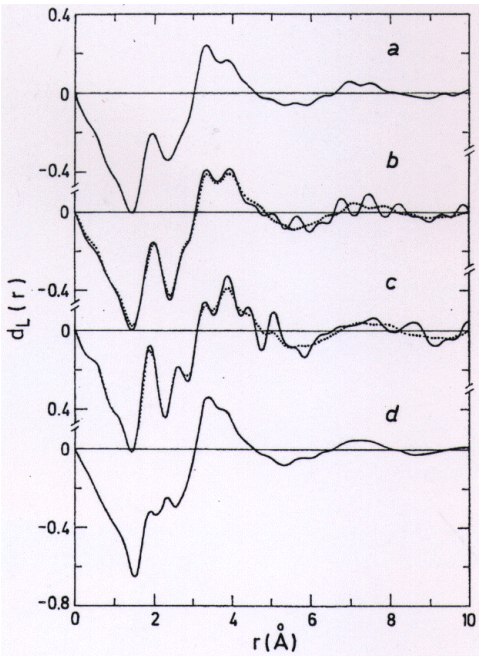

Figure 9. The neutron pair correlation function $d_L(r)$ of water contained in activated carbon, at room temperature, shown by solid lines for 200% (curve a), 42% (curve b) and 25% hydration (curve c). For comparison, the $d_L(r)$ curve of bulk water at the same temperature is also shown (curve d) [29]. The dotted lines correspond to the Fourier transforms of smoothed experimental data. This demonstrates that the additive oscillations that appear between 3 and 6 Å have a physical meaning that is the opposite of the meaning of those appearing at higher r-values.

narrower and shifted to the low values of r, which means that the hydrogen bonding is modified: a peak around 2.65 Å is seen (figure 9(b)). This peak is characteristic of either the O–O or D–D distances; under the two assumptions, this means that the local environment is modified in comparison with what is known for bulk water [4] at the same temperature.

In agreement with previous work [17–19, 23, 30, 31], our study gave support to the existence of a region near the interface where the properties of water are markedly different from those of the bulk phase. It is not possible to determine the thickness of the affected layer. However, a crude determination from the specific area indicates that at some hydration close to 50%, the thickness does not exceed 5 Å. This value must be compared with the computer simulation data [32–38] which indicate that structural modifications do not extend beyond 10 Å from the solid surface.

When partially hydrated samples are cooled down to 77 K, no crystallization peak is detected by differential thermal analysis. X-ray and neutron scattering experiments show that the structure of the amorphous form obtained is different from those of low- and high-density amorphous ices [10–12].

5.3. Biopolymer–water interactions

The structure of water near polymeric membranes [31] has been studied by means of neutron diffraction. Also the structure of water confined in a hydro-gel has been investigated by means of x-ray scattering [39], and the distortion seen at the level of the second-nearest neighbours

attributed to the bending of H bonds. The changes in hydration structure in the active site of unligated glutamate dehydrogenase from Thermococcus profundus have been studied by means of cryogenic x-ray crystal structure analysis and small-angle x-ray scattering [40].

The amount of information available about protein–water correlations is small. For neutron diffraction studies, deuterated samples are required and these are difficult to obtain. However, the first results have been obtained in the case of a photosynthetic C-phycocyanin protein for which the x-ray crystallographic structure is known to a resolution of 1.66 Å [41].

C-phycocyanin is abundant in blue–green algae. Nearly 99%-deuterated samples of this phycobiliprotein were isolated from the cyanobacteria which were grown in perdeuterated cultures [42] (99%-pure D_2O) at Argonne National Laboratory. This process yielded deuterated C-phycocyanin proteins (d-CPC) that had virtually all the ^{1}H–C bonds replaced by ^{2}H–C bonds. One can obtain a lyophilized sample that is similar to amorphous solids as determined by neutron diffraction [31]. As defined in previous papers [48–50], the level of hydration $h = 0.5$ corresponds to 100% hydration of C-phycocyanin which leads to a coverage of about 1.5 monolayers of water molecules on the surface of the protein [44].

The water (D_2O)–protein correlations at the surface of a fully deuterated amorphous protein, C-phycocyanin, have been studied by means of neutron diffraction as functions of temperature and hydration level [31]. The correlation functions $d(r)$ are shown in figure 10 for two levels of hydration of the C-phycocyanin protein. They include both intra-residue and inter-residue correlations. For the 73%-hydrated sample ($h = 0.365$), a definite peak appears at 3.5 Å in $d(r)$. This is the average distance between the centre of mass of a water molecule in the first hydration layer and amino acid residues on the surface of the protein. In the case of the least hydrated sample ($h = 0.175$), the perturbation to the structure of protein due to the water of hydration is not detectable. It is generally assumed in the literature that at full hydration ($h = 0.5$), there is a complete monolayer of water surrounding the protein [46]. For the 73%-hydrated protein, the correlation distance of 3.5 Å measured in these diffraction experiments compared well with computer simulation work on polypeptides and proteins [34, 45] and has been interpreted as resulting from some increase in the clustering of water molecules.

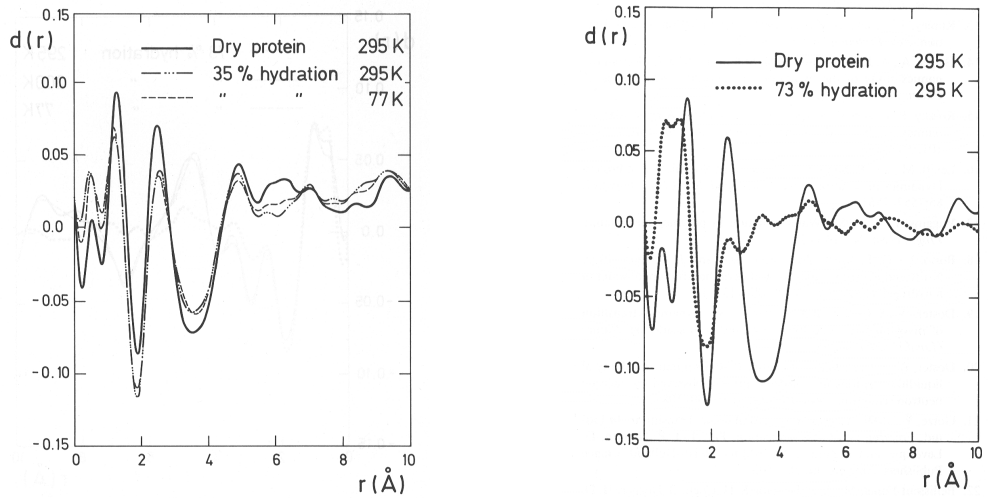

Figure 10. (a) Comparison of $d(r)$ functions for a dry and a 35%-hydrated protein, C-phycocyanin, at room temperature and at 77 K [31]. (b) $d(r)$ functions for a dry deuterated protein, C-phycocyanin, and for a 73%-hydrated protein, C-phycocyanin, at 295 K [31].

Some similarity between the behaviour of water close to C-phycocyanin protein and close to hydrophilic model systems can be stressed. In fact, for low-hydration protein samples, no crystallization of water is detectable, while for more than one-monolayer coverage, hexagonal crystalline ice appears. However, it should be noted that at the highest hydration level, water nucleates into hexagonal ice at low temperature; this is in contrast with the situation for hydrated Vycor, where water nucleates into cubic ice.

Some other interesting findings have come from the study of the glass–liquid transition and the crystallization behaviour of water trapped in loops of methaemoglobin chains [47].

6. Conclusions

From the more recent findings obtained by combining neutron techniques and molecular dynamics simulations, it is now possible to have a more precise picture of water confined in the pores of a hydrophilic porous glass. At room temperature, in the vicinity of a hydrophilic surface, water is in a state equivalent to supercooled bulk water as previously demonstrated; the amount of liquid water depends on the degree of hydration of the sample. Moreover, at room temperature, interfacial water shows a dynamic behaviour similar to that of bulk supercooled water at a temperature 30 K lower [43, 48]. The same trend has been obtained from the study of dynamic properties of water confined in carbon powder [25] as well as at the surface of the C-phycocyanin protein [43, 49].

To conclude, in order to characterize more precisely the nature of the amorphous or liquid phase of water in contact with hydrophilic, hydrophobic or more complex surfaces such as protein surfaces, the site–site partial correlation functions need to be experimentally obtained and compared with those deduced from extended molecular dynamics simulations.

Acknowledgment

The author is pleased to thank S H Chen for his active collaboration in the field of confined water.

References

[1] Bellissent-Funel M-C 1999 *Hydration Processes in Biology: Theoretical and Experimental Approaches* vol 305 (Amsterdam: IOS)
[2] Lovesey S W 1987 *Theory of Neutron Scattering from Condensed Matter* 3rd edn (Oxford: Clarendon)
[3] Dore J C 1985 *Water Science Reviews* vol 1, ed F Franks (Cambridge: Cambridge University Press)
[4] Bellissent-Funel M-C 1991 *Hydrogen Bonded Liquids (NATO ASI Series C)* ed J C Dore and J Teixeira (Dordrecht: Kluwer Academic)
[5] Bellissent-Funel M-C, Bosio L and Teixeira J 1991 *J. Phys.: Condens. Matter* **3** 4065
[6] Chen S H and Teixeira J 1985 *Adv. Chem. Phys.* **64** 1
[7] Bellissent-Funel M-C and Bosio L 1995 *J. Chem. Phys.* **102** 3727 and references therein
[8] Bellissent-Funel M-C, Tassaing T, Zao H, Beysens D, Guillot B and Guissani Y 1997 *J. Chem. Phys.* **107** 2942
[9] Hobbs P V 1974 *Ice Physics* (Oxford: Clarendon)
[10] Bizid A, Bosio L, Defrain A and Oumezzine M 1987 *J. Chem. Phys.* **87** 2225
[11] Bellissent-Funel M-C, Teixeira J and Bosio L 1987 *J. Chem. Phys.* **87** 2231
[12] Bellissent-Funel M-C, Bosio L, Hallbrucker A, Mayer E and Sridi-Dorbez R 1992 *J. Chem. Phys.* **97** 1282
[13] Angell C A 1981 *Water: a Comprehensive Treatise* vol 7, ed F Franks (New York: Plenum) ch 1
[14] Bellissent-Funel M-C, Teixeira J, Bosio L and Dore J C 1989 *J. Phys.: Condens. Matter* **1** 7123
[15] Hawkins R K and Egelstaff P A 1980 *Clays Clay Minerals* **28** 19
[16] Soper A K 1991 *Hydrogen-Bonded Liquids* vol 329, ed J C Dore and J Teixeira (Dordrecht: Kluwer Academic) p 147
[17] Steytler D C and Dore J C 1985 *Mol. Phys.* **5** 1001

[18] Dore J C, Dunn M and Chieux P 1987 *J. Physique Coll.* **48** C1 457
[19] Dore J C, Coveney F and Bellissent-Funel M-C 1992 *Recent Developments in the Physics of Fluids* ed W S Howells and A K Soper (Bristol: Institute of Physics Publishing) p 299
[20] Benham M J, Cook J C, Li J C, Ross A D K, Hall P L and Sarkissian B 1989 *Phys. Rev.* B **39** 633
[21] Venuti V, Crupi V, Magazu S, Majolino D, Migliardo P and Bellissent-Funel M-C 2000 *J. Physique* IV **10** Pr7 211
[22] Smirnov P, Yamaguchi T, Kittaka S, Takahara S and Kuroda Y 2000 *J. Phys. Chem.* B **23** 5498
[23] Bellissent-Funel M-C, Bosio L and Lal J 1993 *J. Chem. Phys.* **98** 4246
[24] Chen S H and Bellissent-Funel M C 1994 *Hydrogen Bond Networks (NATO ASI Series C, vol 435)* ed M-C Bellissent-Funel and J C Dore (Dordrecht: Kluwer Academic) p 307
[25] Zanotti J-M 1997 *PhD Thesis* Orsay University, France
[26] General information on Vycor-brand porous 'Thirsty Glass', No 7930, Corning Glass Works, is available from OEM Sales Service, Box 5000, Corning, NY 14830, USA
[27] Bruni F, Ricci M A and Soper A K 1998 *J. Chem. Phys.* **109** 1478
[28] Ricci M A, Bruni F, Gallo P, Rovere M and Soper A K 2000 *J. Phys.: Condens. Matter* **12** A345
[29] Bellissent-Funel M-C, Sridi-Dorbez R and Bosio L 1996 *J. Chem. Phys.* **104** 10 023
[30] Wiggins P M 1988 *Prog. Polym. Sci.* **13** 1
[31] Bellissent-Funel M-C, Lal J, Bradley K F and Chen S H 1993 *Biophys. J.* **64** 1542
[32] Lee C Y, McCammon J A and Rossky P J 1984 *J. Chem. Phys.* **80** 4448
[33] Lee S H and Rossky P J 1987 *Proc. 10th Korean Scientists and Engineers Conf.* (Seoul, Korea: Inchen) p 150
[34] Levitt M and Sharon R 1988 *Proc. Natl Acad. Sci. USA* **85** 7557
[35] Rossky P J and Lee S H 1989 *Chem. Scr.* A **29** 93
[36] Lee S H and Rossky P J 1994 *J. Chem. Phys.* **100** 3334
[37] Rossky P J 1994 *Hydrogen Bond Networks (NATO ASI Series C, vol 435)* ed M-C Bellissent-Funel and J C Dore (Dordrecht: Kluwer Academic) p 337
[38] Alary F, Durup J and Sanejouand Y-H 1993 *J. Phys. Chem.* **97** 13 864
[39] Bosio L, Johari G P, Oumezzine M and Teixeira J 1992 *Chem. Phys. Lett.* **188** 113
[40] Nakasako M, Fujisawa T, Adachi S, Kudo T and Higuchi S 2001 *Biochemistry* **40** 3069
[41] Duerring M, Schmidt G B and Huber R 1987 *J. Mol. Biol.* **217** 577
[42] Crespi H L 1977 *Stable Isotopes in the Life Sciences* vol 111 (Vienna: IAEA)
[43] Bellissent-Funel M-C, Zanotti J-M and Chen S H 1996 *Faraday Discuss.* **103** 281
[44] Middendorf H D 1995 *Nonlinear Excitations in Biomolecules* ed M Peyrard (Les Ulis: Les Editions de Physique) p 369
[45] Rossky P J and Karplus M 1979 *J. Am. Chem. Soc.* **101** 1913
[46] Lee B and Richard F M 1971 *J. Mol. Biol.* **55** 379
[47] Sartor G, Hallbrucker A, Hofer H and Mayer E 1993 *Proc. Conf. on Water–Biomolecule Interactions* (Bologne: SIF) pp 143–6
[48] Bellissent-Funel M-C, Longeville S, Zanotti J-M and Chen S H 2000 *Phys. Rev. Lett.* **85** 3644
[49] Dellerue S and Bellissent-Funel M-C 2000 *Chem. Phys.* **258** 315
[50] Levitz P, Ehret G, Sinha S K and Drake J M 1991 *J. Chem. Phys.* **96** 6151